Xanthine Quartets on Au(111)

Chong Chen,[†,‡,] Hongqian Sang,[§,] Pengcheng Ding,[⊥,] Ye Sun,[⊥] Manuela Mura,[¶] Ying Hu,[#] Lev N. Kantorovich,[*,∥] Flemming Besenbacher,[*,‡] and Miao Yu[*,†]

[†]School of Chemistry & Chemical Engineering, Harbin Institute of Technology, Harbin 150001, China
[‡]iNANO and Department of Physics and Astronomy, Aarhus University, Aarhus 8000, Denmark
[§]Institute for Interdisciplinary Research, Jianghan University, Wuhan 430056, China
[∥]Department of Physics, King's College London, The Strand, London WC2R 2LS, United Kingdom
[⊥]Condensed Matter Science and Technology Institute, Harbin Institute of Technology, Harbin 150001, China
[#]School of Life Science and Technology, Harbin Institute of Technology, Harbin 150001, China
[¶]School of Mathematics and Physics, University of Lincoln, Brayford Pool LN6 7TS, United Kingdom

ABSTRACT: The quartet of xanthine (X), a purine base ubiquitously distributed in most human body tissues and fluids, has been for the first time fabricated and visualized, as the first alternative purine quartet besides the known guanine (G)-quartet. The X-quartet network is demonstrated to be the most stable phase on Au(111). Unlike guanine, the fabrication of the X-quartets is not dependent on the presence of metal atoms, which makes it the first metal-free purine quartet. The X-quartet holds great promise to potentially construct artificial new DNA quadruplexes for genetic regulation and antitumor therapy. Moreover, both the X-quartet itself and the quartet networks favor homochirality, suggesting homochiral xanthine oligomers and the networks may have been formed as the precursors of the pristine oligonucleotides on primitive Earth.

As a noncanonical secondary formation of DNA sequences, DNA quadruplexes have sparked tremendous interest in the biological and medical societies, due to their paramount importance in homologous recombination, DNA replication, transcriptional regulation, chromosome stability, and high therapeutic potentials.[1−5] Albeit ample speculation on a possibility of various quadruplexes, the only one whose presence has been explicitly confirmed is the guanine (G)-quadruplex, composed of stacking G-quartets with monovalent cations coordinated in between. It has been revealed formation and stabilization of G-quadruplexes are exceptionally dependent on the incorporated metal ions.[1,2,6,7]

Xanthine (3,7-dihydro-purine-2,6-dione, X) is a purine base ubiquitously distributed in most human body tissues and fluids as well as in other organisms. As an intermediate in nucleic acid degradation, xanthine can be generated *in vivo* from guanine by deamination.[8−11] Very promisingly, recent results based on mass spectroscopy, nuclear magnetic resonance spectroscopy and quantum chemical computations proposed xanthine and its derivatives have the potential to be an alternative candidate to form stable quartets,[7,12] whereas molecular dynamics simulations further suggested the high degree of structural and energetic compatibility of X-quartet may lead to new quadruplexes by replacing G-quartets with X-quartets.[13] However, definitive experimental evidence, confirming the existence of the X-quartets, has been still lacking.

In the biological world, homochirality is common in amino acids, protein, carbohydrates and their assemblies.[14] It is suggested extended homochiral networks of nucleobases may have been formed on montmorillonite clay by oligomerization under prebiotic conditions.[15,16] Xanthine is prochiral, forming two enantiomers when adsorbed in either "face-up" or "face-down" geometry. Considering xanthine is one of the original nucleobases in prebiotic Earth[17,18] and found abundant in meteorites from outer space,[19] the conformation of X-oligomer and the chirality of X-networks must be extraordinarily intriguing for understanding prebiotic synthesis of nucleic acid, which is fundamental to origin of life.

Herein, X-quartet has been fabricated and visualized for the first time (Scheme 1). Based on *in situ* thermodynamic investigation and the calculated stabilization energies, the quartet network is confirmed to be the most stable phase of xanthine on Au(111). Importantly, in contrast to guanine, it is revealed formation of the X-quartet is not dependent on the participation of metal atoms. Moreover, the quartets are homochiral, composed by either of the two xanthine

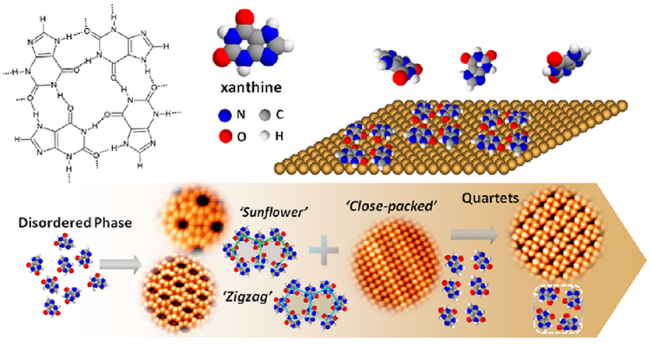

Scheme 1. Illustration of a Xanthine Quartet and the Thermodynamic Transformation of Xanthine on Au(111)

enantiomers. Interestingly, both the quartet itself and the 2-D assembly of the quartets prefer homochirality. This work demonstrates a potential for xanthine to construct quartets hence artificial new DNA quadruplexes, which may find various applications in genetic regulation and antitumor therapy, meanwhile indicates homochiral X-based oligo-nucleotides might have been prevailing at early stages of life.

When sublimated xanthine molecules are deposited on Au(111) kept at room temperature (RT), well-ordered extended 2-D islands can be obtained upon 20 min postannealing at 430 K (details in the Supporting Information (SI)). From the scanning tunneling microscopy (STM) results scanned at RT, the surface corrugation corresponding to the herringbone reconstruction of the pristine Au(111) remains unchanged, indicating the weak molecule−substrate interaction. Each individual xanthine molecule appears as a quasi-triangular protrusion (Figure 1a), and every four xanthines form

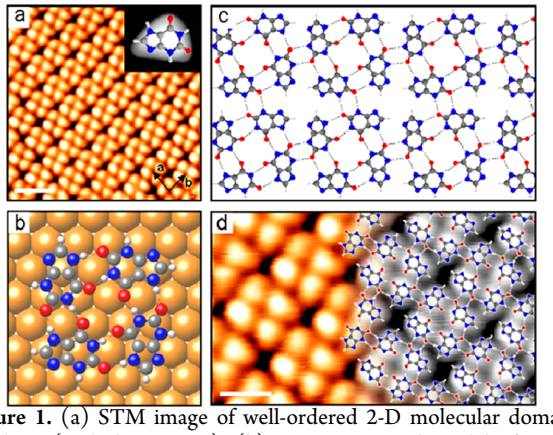

Figure 1. (a) STM image of well-ordered 2-D molecular domain of xanthine (scale bar: 2 nm). (b) DFT optimized model of xanthine quartet on Au(111). (c) DFT calculated network of xanthine quartets. (d) Close view of quartet network, with proposed DFT model superimposed (scale bar: 1 nm).

a typical quartet. Direct indication for the existence of individual quartets can be found at the step edges of Au(111) (Figure S1a,b) as well as the edges of quartet domains (Figure S1c,d). The formation of X-quartets was further explored by density functional theory (DFT) calculations. It is revealed a xanthine molecule is adsorbed flatly on Au(111) at a vertical distance of 3.5 Å. The four xanthines in a single quartet are stabilized by double N−H···O hydrogen bonds, with a total binding energy of 2.93 eV (Figure 1b). No charge transfer is found between the adsorbed xanthine and Au, and the xanthine interaction with the surface is almost independent of its actual position on it. Justified by this fact, we then simulated the network in the gas phase. Besides the inner-quartet bonds, additional double N−H···O hydrogen bonds between neighboring quartets stabilize the quartet network (Figure 1c), resulting a binding energy of 4.88 eV for each unit cell. Moreover, it is demonstrated the dimension of the calculated unit cell is 1.374 nm × 1.374 nm, consistent with the experimental results (Figure 1d).

Although *in vivo* results would be more preferred, the direct visualization of the X-quartets on Au(111) in UHV is already a significant achievement, because (1) a weak interaction with the substrate allows formation of the quartet to be essentially determined by the intermolecular interaction with little influence of the substrate; (2) the UHV conditions help in forming the network without disturbance of contaminants; (3) adsorption and assembly of xanthine on inorganic grains may have played crucial role in biosynthesis at prebiotic stage.[17]

For in-depth understanding of the formation of X-quartet and the *in situ* thermodynamic transformation, the adsorption of xanthine was investigated at different annealing temperatures. Single-layer domains of close-packed xanthine molecules without periodicity are obtained at RT (Figure 2a). Upon

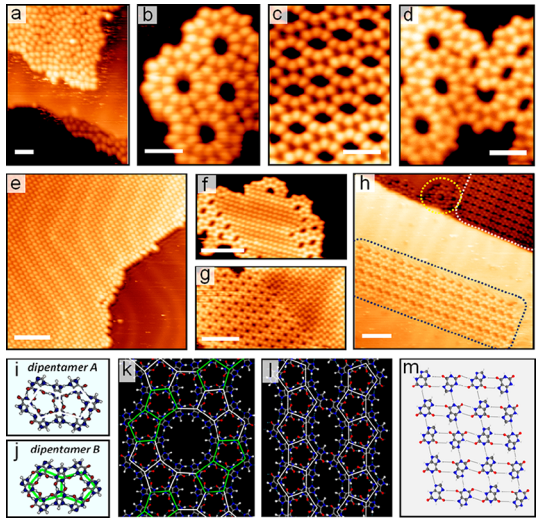

Figure 2. Xanthine structural phases formed on Au(111) at various temperatures. (a) Room temperature structure; (b) "*Sunflower*" phase; (c) "*Zigzag*" phase; (d) "*Sunflower*"−"*Zigzag*" combination; (e) "*Close-packed*" phase; (f) combined "*Sunflower*", "*Zigzag*" and "*Close-packed*" phase; (g) joint domain of "*Close-packed*" and quartet phase; and (h) coexistence of "*Sunflower*", "*Zigzag*" and quartet structures, outlined in yellow, blue and white, respectively. (i) "*dipentamer-A*" and (j) "*dipentamer-B*" of xanthine. (k−m) Calculated models of "*Sunflower*", "*Zigzag*" and "*Close-packed*" structures, where "*dipentamer-A*" and "*dipentamer-B*" are marked in white and green (scale bar: 2 nm in panels a−d; 5 nm in panels e−h).

temperature rise, this disordered arrangement is gradually modified by forming tiny patches of ordered rows and random five-molecule units (quintets) in the domains. When the temperature is increased above 350 K, small islands of two ordered phases referred as "*Sunflower*" (Figure 2b) and "*Zigzag*"[20] (Figure 2c) start to appear and coexist with the disordered region. The two phases can form both separated domains and mixed islands (Figure 2d). Accompanying these two phases, the third ordered structure, i.e. the "*Close-packed*" phase (Figure 2e), is found. Besides the islands of single phase, the "*Sunflower*" and "*Zigzag*" can decorate the edges of the "*Close-packed*" to form a joint domain (Figure 2f). The domination of the three phases becomes more pronounced at higher annealing temperatures with shrinking and finally vanishing of the disordered portion. Until 423 K, the X-quartet phase emerges, and the four phases coexist (Figure 2g,h).

The stability of the 2-D phases was then analyzed theoretically. It is revealed both "*Sunflower*" and "*Zigzag*" structures are tiled by xanthine dipentamers (Figure 2i,j), with the former composed of both "*dipentamer A*" and "*dipentamer B*" (Figure 2k), and the latter formed exclusively by one of them (Figure 2l and S2). In both phases, every xanthine molecule in the network interacts with its three neighbors by three pairs of double hydrogen bonds. The binding energy of the two phases is identical, which is 1.09 eV per molecule. For the "*Close-*

packed" phase (Figure 2m), every molecule interacts with its nearest four neighbors by two pairs of double N−H···O bonds within the horizontal row and two single N−H···N bond between the rows, with a formation energy of 1.16 eV. A rather interesting fact is each molecule in all the four phases has six hydrogen bonds with neighbors. The quartet phase has the highest binding energy (1.22 eV per molecule), consistent with the experimental observation the quartet structure is formed at a higher temperature than that of other phases. Especially, at 430 K, the quartet network presents as the only form on the surface (Figure S3a). Finally, at a slightly higher temperature (433 K), all molecules are desorbed from the substrate (Figure S3b).

Given the fact the G-quadruplex is the only quadruplex directly visualized so far,[21] it is intriguing to compare G-quartet with X-quartet on Au(111). X-quartet is stabilized by eight N−H···O bonds, whereas G-quartet by four N−H···O and four N−H···N bonds. Albeit the slightly higher stabilization energy of xanthine dimer (0.75 eV) in X-quartet than that of the guanine dimer (0.67 eV, Figure 3a), G-quartet shows a higher stabilization energy than X-quartet (Figure 3b), i.e., 0.89 vs 0.73 eV per molecule, due to the additional cooperativity effect of the former.[7,22]

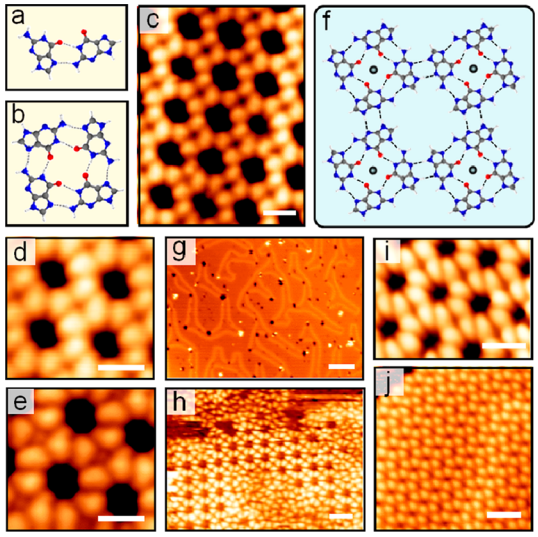

Figure 3. (a) Dimer and (b) quartet of guanine. (c−e) Large-scale and close-view of guanine−Na network, with Na invisible/visible in the quartet center. (f) DFT calculated model of porous network tiled by guanine−Na complexes. (g) Specially prepared Au substrate with plenty of defects, where herringbone reconstruction is seriously varied together with ample holes on the terraces. (h) Assembly of guanine on the defect-rich Au substrate at 340 K. (i) Ordered porous network of G-Au units. (j) High-temperature structural phase of guanine (scale bar: 1 nm in panels c−e; 10 nm in panel g; 2 nm in panels h−j).

A surprising fact is it is difficult to get G-quartets on well-defined defect-free Au(111) without additional metal atoms (see SI). As comparison, well-ordered networks composed of quartet-like motifs can be easily formed for guanine-Na at 320 K (Figure 3c), in good agreement with the guanine assembly with K.[23] In most cases, the metal atoms in guanine-metal complex are invisible (Figure 3d), and only emerge in the images under special tip conditions (Figure 3e). Known from the calculated model (Figure 3f), together with the four pairs of double hydrogen bonds, the quartet is further stabilized by the Na−carbonyl interaction, and linked to neighbors by double N−H···N bonds.

Given the inertness of Au and physisorption of guanine on Au(111), the contribution of Au adatoms from the substrate was not been considered in our earlier work.[22] Very strikingly, it is revealed even adatoms from the Au substrate can induce G-quartets. By applying a harsh sputtering with a mild annealing, the perfection of Au surface is compromised to produce plenty of defects (Figure 3g and S5) and hence facilitate the generation of Au adatoms. When guanine is deposited on such surface without annealing, disordered structure is found (Figure S6). When the temperature is increased to 333 K, individual quartet-like units start to show at the edge of disordered domains (Figure S7). At 340 K, typical porous networks composed of quartet units like that of G−Na assembly are formed, together with randomly packed guanines (Figure 3h and S8). The percentage of the porous network can be raised at higher temperatures (Figure 3i and S9). Once the well-defined ordering of the Au substrate is compromised, it takes long-term treatments to restore. Before full recovery, quartet-like motifs can still be observed. All the results indicate the metal atoms play an important role in the formation of the quartets. Concurringly, it has been revealed by *in vivo* experiments and former theoretical calculations the contribution of the monovalent cations is indispensable for the formation and stabilization of the G-quadruplex, and the absence of these ions can lead to a lower stability and even complete decomposition.[1,2,6,7] Moreover, the G-Au quartet is converted into the "*high-temperature*" phase like that of pure guanines at 350 K until full desorption (Figure 3j).

As a sharp contrast, the participation of Au adatoms in the formation of X-quartet can be essentially excluded based on the following facts: (1) X-quartet can already form on defect-free Au substrate whereas G-quartet cannot; (2) there is no modification of herringbone reconstruction, or emerged holes/islands, or varied step edges found after the formation of X-quartet, indicating barely any migration of Au atoms. Therefore, the formation of X-quartet does not require metals, consistent with the former calculated results, showing X-quadruplexes are stable without intercalating ions.[12]

Calculation results reveal the X-quartets must be homochiral composed of either four left-handed "S-xanthine" or four right-handed "R-xanthine" (Figure 4a, details in SI). Both quartets networks (denoted as "S-X-quartet" and "R-X-quartet") have been observed on the surface. A statistical analysis of STM images shows the proportion of the two quartets is nearly identical. Moreover, the quartet networks are also homochiral, i.e. tiled exclusively by only one of the two quartets. Domains of different chiralities can merge without forming defects at the boundary (Figure 4b-4d). Rarely individual quartets with different handedness can also participate in the quartet network as "defects" (Figure 4e). It is revealed neighboring S- and R-quartets are also bonded by double hydrogen bonding, i.e., one N−H···O and one N−H···N. Moreover, although the presence of such an individual quartet with an opposite handedness (Figure 4f) may contribute to the slightly increased entropy and hence lower its free energy, the mixture suffers a DFT energy penalty of 0.68 eV that easily compensates for this effect (see SI).

In summary, we have produced and directly visualized X-quartets and their networks for the first time. Among all 2-D architectures, the quartet network is the most stable phase with the highest stabilization energy. Both the high stability and the

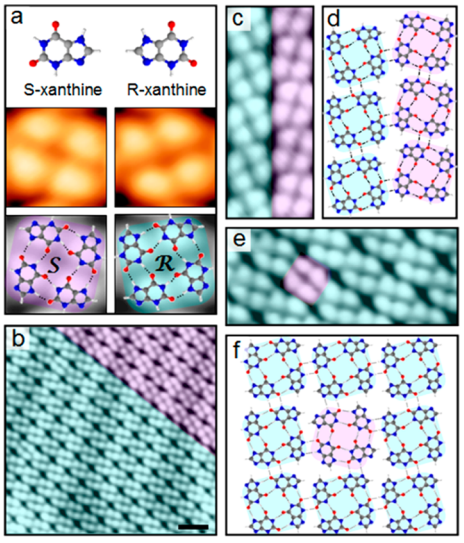

Figure 4. (a) STM results of individual homochiral X-quartets comprising either four left-handed S- (S-X-quartet) or four right-handed R- (R-X-quartet) enantiomers with superimposed calculated models, marked in purple and blue, respectively. (b) Large scale STM image of X-quartets network, containing a S-X-quartets domain (in purple) side-by-side with a R-X-quartet domain (in blue), displaying no defects at interface (scale bar: 2 nm). (c) Zoom-in image and (d) calculated gas-phase model of neighboring S- and R-quartet rows. (e) STM image and (f) calculated model for case where an individual quartet with an opposite handedness intercalates in the quartet network.

planarity of this new quartet make it a promising candidate for constructing artificial quadruplexes. Deeper insight has been achieved for the quartet-like formation of guanine on Au(111), revealing both the extraneous metal atoms and the Au adatoms can induce the quartet-like motifs, but not quartets can be obtained without metal atoms. In contrast, the fabrication of the X-quartets is not dependent on the presence of metal atoms. Given its distinction from the G-quartet, X-quartet then holds great promise to provide versatility and flexibility for the biochemical synthesis of artificial quadruplexes.

We also find homochriality is overwhelmingly present for individual quartets. Although it is possible to mix the quartets of different handedness in the networks, homochiral networks tiled exclusively by quartets of single handedness are greatly abundant. The results imply the selection of homochirality may have occurred at early stages of life, and such homochiral xanthine oligomers and the networks may have been formed on clay and other grain surfaces and serve as the precursors of the pristine oligonucleotides on primitive Earth.

■ ACKNOWLEDGMENTS

This work is financially supported by the National Natural Science Foundation of China (21473045, 51401066).

■ REFERENCES

(1) Bochman, M. L.; Paeschke, K.; Zakian, V. A. *Nat. Rev. Genet.* **2012**, *13*, 770−780.
(2) Balasubramanian, S.; Hurley, L. H.; Neidle, S. *Nat. Rev. Drug Discovery* **2011**, *10*, 261−275.
(3) Huang, F. W.; Hodis, E.; Xu, M. J.; Kryukov, G. V.; Chin, L.; Garraway, L. A. *Science* **2013**, *339*, 957−959.
(4) Horn, S.; Figl, A.; Rachakonda, P. S.; Fischer, C.; Sucker, A.; Gast, A.; Kadel, S.; Moll, I.; Nagore, E.; Hemminki, K.; Schadendorf, D.; Kumar, R. *Science* **2013**, *339*, 959−961.
(5) Dilley, R. L.; Verma, P.; Cho, N. W.; Winters, H. D.; Wondisford, A. R.; Greenberg, R. A. *Nature* **2016**, *539*, 54−58.
(6) Špačková, N.; Berger, I.; Šponer, J. *J. Am. Chem. Soc.* **1999**, *121*, 5519−5534.
(7) Paragi, G.; Kovács, L.; Kupihár, Z.; Szolomájer, J.; Penke, B.; Guerra, C. F.; Bickelhaupt, F. M. *New J. Chem.* **2011**, *35*, 119−126.
(8) Singer, B.; Grunberger, D. Plenum Press: New York, 1983.
(9) Vongchampa, V.; Dong, M.; Gingipalli, L.; Dedon, P. *Nucleic Acids Res.* **2003**, *31*, 1045−1051.
(10) Hollstein, M.; Sidransky, D.; Vogelstein, B.; Harris, C. *Science* **1991**, *253*, 49−53.
(11) David, S. S.; O'Shea, V. L.; Kundu, S. *Nature* **2007**, *447*, 941−950.
(12) Szolomájer, J.; Paragi, G.; Batta, G.; Guerra, C. F.; Bickelhaupt, F. M.; Kele, Z.; Pádár, P.; Kupihár, Z.; Kovács, L. *New J. Chem.* **2011**, *35*, 476−482.
(13) Novotný, J.; Kulhánek, P.; Marek, R. *J. Phys. Chem. Lett.* **2012**, *3*, 1788−1792.
(14) Chen, C.; Wang, D.; Wan, L. J. *Nat. Sci. Rev.* **2015**, *2*, 205−216.
(15) Joshi, P. C.; Aldersley, M. F.; Delano, J. W.; Ferris, J. P. *J. Am. Chem. Soc.* **2009**, *131*, 13369−13374.
(16) Ferris, J. P.; Ertem, G. *Science* **1992**, *257*, 1387−1389.
(17) Sowerby, S. J.; Petersen, G. B. *Origins Life Evol. Biospheres* **1999**, *29*, 597−614.
(18) Sowerby, S. J.; Cohn, C. A.; Heckl, W. M.; Holm, N. G. *Proc. Natl. Acad. Sci. U. S. A.* **2001**, *98*, 820−822.
(19) Callahan, M. P.; Smith, K. E.; Cleaves, H. J.; Ruzicka, J.; Stern, J. C.; Glavin, D. P.; House, C. H.; Dworkin, J. P. *Proc. Natl. Acad. Sci. U. S. A.* **2011**, *108*, 13995−13998.
(20) Yu, M.; Wang, J. G.; Mura, M.; Meng, Q. Q.; Xu, W.; Gersen, H.; Lægsgaard, E.; Stensgaard, I.; Kelly, R. E. A.; Kjems, J.; Linderoth, T. R.; Kantorovich, L. N.; Besenbacher, F. *ACS Nano* **2011**, *5*, 6651−6660.
(21) Biffi, G.; Tannahill, D.; McCafferty, J.; Balasubramanian, S. *Nat. Chem.* **2013**, *5*, 182−186.
(22) Otero, R.; Schöck, M.; Molina, L. M.; Laegsgaard, E.; Stensgaard, I.; Hammer, B.; Besenbacher, F. *Angew. Chem., Int. Ed.* **2005**, *44*, 2270−2275.
(23) Xu, W.; Wang, J. G.; Yu, M.; Lægsgaard, E.; Stensgaard, I.; Linderoth, T. R.; Hammer, B.; Wang, C.; Besenbacher, F. *J. Am. Chem. Soc.* **2010**, *132*, 15927−15929.